PNAS RESEARCH ARTICLE | MICROBIOLOGY
APPLIED PHYSICAL SCIENCES

Porphyrin nanoemulsion for antimicrobial photodynamic therapy: effective delivery to inactivate biofilm-related infections

Hilde Harb Buzzá[a,b], Fernanda Alves[a], Ana Julia Barbosa Tomé[a], Juan Chen[c], Giulia Kassab[a], Jiachuan Bu[c], Vanderlei Salvador Bagnato[a,d,1], Gang Zheng[c,e,1], and Cristina Kurachi[a,1]

Edited by; received September 22, 2022; accepted September 29, 2022

The management of biofilm-related infections is a challenge in healthcare, and antimicrobial photodynamic therapy (aPDT) is a powerful tool that has demonstrated a broad-spectrum activity. Nanotechnology has been used to increase the aPDT effectiveness by improving the photosensitizer's delivery properties. NewPS is a simple, versatile, and safe surfactant-free nanoemulsion with a porphyrin salt shell encapsulating a food-grade oil core with promising photodynamic action. This study evaluated the use of NewPS for aPDT against microorganisms in planktonic, biofilm, and in vivo models of infected wounds. First, the potential of NewPS-mediated aPDT to inactivate *Streptococcus pneumoniae* and *Staphylococcus aureus* suspensions was evaluated. Then, a series of protocols were assessed against *S. aureus* biofilms by means of cell viability and confocal microscopy. Finally, the best biofilm protocol was used for the treatment of *S. aureus* in a murine-infected wound model. A high NewPS-bacteria cell interaction was achieved since 0.5 nM and 30 J/cm^2 was able to kill *S. pneumoniae* suspension. In the *S. aureus* biofilm, enhanced efficacy of NewPS-aPDT was achieved when 100 μM of NewPS was applied with longer periods of incubation at the light dose of 60 J/cm^2. The best single and double-session protocol reduced 5.56 logs and 6.03 logs, respectively, homogeneous NewPS distribution, resulting in a high number of dead cells after aPDT. The in vivo model showed that one aPDT session enabled a reduction of 6 logs and faster tissue healing than the other groups. In conclusion, NewPS-aPDT may be considered a safe and effective anti-biofilm antimicrobial photosensitizer.

nanoemulsion | antimicrobial photodynamic therapy | biofilm | *Staphylococcus aureus* | *Streptococcus pneumoniae*

Significance

The porphyrin nanoemulsion showed effective performance as photosensitizer delivery formulation in the three investigated bacterial models. A high interaction with planktonic *Staphylococcus aureus* was evident by the significant inactivation results even at the nanomolar range. At the biofilm, bacteria reduction of 6 log was achieved, proving its efficient delivery even at a protective extracellular matrix structure. Finally, the porphyrin nanoemulsion was also effective in the infected ulcer model, overcoming the biological complexity present at infected tissues that limits photosensitizer uptake by the microorganism.

Infections caused by bacteria are one of the major problems for humanity. Even when the microorganisms are commensal of the human microbial flora, changes in the host immune system or locally in the tissue environment may result in their pathogenic action for the development of a large number of severe diseases. *Staphylococcus aureus* and *Streptococcus pneumoniae* are commonly found in the human body and are among the most dangerous strains from a clinical aspect (1, 2). This scenario tends to worsen if actions are not taken, mainly because of the ability of these microorganisms to develop resistance or tolerance to the available antibiotics, leading to high rates of failure in the treatment (3). Alternative treatments to antibiotics and development of improved drug delivery systems are two of the urgent actions to take to overcome the antimicrobial resistance (AMR) global consequences. In addition to the AMR, the biofilm formation ability of some bacteria species is also considered a protection mechanism from physical, chemical, and environmental stress.

Biofilm is a very complex community of microorganisms, highly structured and involved in an extracellular matrix (ECM) that is attached to a biotic or abiotic surface. The human body presents surfaces that are attractive niches for microbial adhesion and growth, resulting in an interface that serves as reservoirs for biofilm development (4–6). It is also considered one of the most widely spread and successful modes of life on the Earth, and it is the most predominant microbial lifestyle in natural environments. Studies have shown that biofilms are more resistant in drastic conditions as when under ultraviolet radiation, extreme temperature and pH levels, high salinity, high pressure, poor nutrients, and treatment response with a range of antibiotics. In addition, 70–75% of the human infections are related to microorganisms organized in biofilms, which are more resistant to treatments than their planktonic counterparts (4–6). Therefore, an efficient antimicrobial treatment must provide microorganism inactivation in both the planktonic and biofilm forms, as well as in a much more complex biological environment of the infected tissue. Additionally, any clinical treatment must be safe, in

Author contributions: H.H.B., F.A., J.C., G.K., V.B., G.Z., and C.K. designed research; H.H.B., F.A., A.J.B.T., J.C., G.K., and J.B. performed research; H.H.B. and F.A. contributed new reagents/analytic tools; H.H.B., F.A., A.J.B.T., J.C., G.K., V.S.B., G.Z., and C.K. analyzed data; H.H.B., F.A., J.C., G.K., V.S.B., G.Z., and C.K. wrote the paper; G.Z. and C.K. conducted the study; and V.S.B., G.Z. and C.K. performed experiment idealization.

The authors declare no competing interest.

This article is a PNAS Direct Submission.

Copyright © 2022 the Author(s). Published by PNAS. This article is distributed under Creative Commons Attribution-NonCommercial-NoDerivatives License 4.0 (CC BY-NC-ND).

[1]To whom correspondence may be addressed. Email: vander@ifsc.usp.br, gang.zheng@uhnres.utoronto.ca, or cristina@ifsc.usp.br.

This article contains supporting information online at http://www.pnas.org/lookup/suppl/doi:10.1073/pnas.2216239119/-/DCSupplemental.

Published November 8, 2022.

Downloaded from https://www.pnas.org by Escola Sup Agricultura - USP on November 16, 2022 from IP address 143.107.180.158.

this case, must not induce relevant side effects for the host organism. In other words, the antimicrobial treatment must result in the inactivation of the pathogenic microorganisms without damaging the host tissues.

An alternative technique applied in the treatment of various infection diseases is antimicrobial photodynamic therapy (aPDT) (7). Its mechanism of action is based on the interaction of three fundamental elements: light at an appropriate wavelength, a photosensitive molecule, called photosensitizer (PS), and the presence of molecular oxygen. The interaction between light and the photosensitizer results in physical–chemical reactions that generate reactive species of oxygen with high oxidation power of the cellular components (8, 9). Specifically, for the case of aPDT, the photosensitizer molecules must be attached to the cell wall or internalized in the microorganism cells. The photodynamic action only takes place in the microscopic vicinity of the photosensitizer molecule, and a certain threshold value must be achieved, meaning photosensitizer concentration and light fluence (J/cm^2) in the target microorganism, to result in cell death.

The aPDT has demonstrated a broad spectrum of activity against bacteria including both drug-sensitive and drug-resistant pathogens (10). However, studies have shown that biofilms are less susceptible to PDT than planktonic cells (11) even with the use of different photosensitizer classes. For aPDT to be efficient in biofilm, the photosensitizer molecules have to be globally and homogenously distributed within all layers from the surface up to the adhered interface (12–14). Biofilm ECM plays a relevant role preventing free diffusion of the drug molecules, decreasing their mobility, especially to the deep layers, resulting in a gradient photosensitizer concentration and partial inactivation response. Considering a clinical scenario, if the cells are not inactivated, the released viable ones may adhere to other surfaces beginning the growing of other biofilm communities or infection sites. Some photosensitizer characteristics, such as low solubility, decreased tissue penetration, low specificity, and low accumulation in the target cells, are limitations that should be overcome (15). When considering an infected tissue, the microorganisms are present at an overlaying biofilm but also pathogen cells can invade the tissue and being intermingled between the host cells. This is a much more complex biological system to efficiently deliver the photosensitizer to the microorganism cells.

For these reasons, the photosensitizer delivery has a great influence on the photodynamic efficacy, and its formulation and design may be specifically designed to overcome the challenges for antimicrobial response in such distinct biological environments. Nanotechnology has been used to increase the effectiveness of molecules with poor pharmacokinetics and pharmacodynamics properties, including photosensitizer (16). Specifically, it has demonstrated therapeutic improvement in drug penetration within biofilms, increasing the diffusion of the active molecule through the extracellular matrix, resulting in higher drug (photosensitizer) delivery to the microorganism and a higher cellular retention (17, 18).

We recently developed a surfactant-free nanoemulsion with a porphyrin salt shell encapsulating a food-grade oil core capable of coloading antibiotics, making it simple, versatile and safe. Called NewPS, it has a ~120 nm spherical structure and negative charge surface (zeta potential, –25 mV). It exhibits excellent colloidal stability across wide temperature ranges (4–100 °C), pH range (4–12), and mechanical agitation (80,000 g). NewPS was originally designed for systemic delivery but encountered the challenge of fast blood clearance (19). Here, we hypothesize that the high PS packing capacity of NewPS in the form of oil-in-water emulsion (>10 wt%) together with its remarkable colloidal stability and antibiotics codelivery potential makes it perfect for topical application to combat photosensitizer penetration challenges in biofilm treatment. Taking these promising aspects of the nanoemulsion, this study evaluated the use of NewPS for aPDT against the three forms of microorganisms: planktonic, biofilm, and in vivo model with infected wounds.

Results

Antimicrobial Photodynamic against Planktonic Form of *S. pneumoniae* and *S. aureus*. NewPS was formulated by the self-assembly of pyropheophorbide α monosodium salt around a glyceryl trioctanoate oil core according to a previously published method (19). The morphology of the formed NewPS was disclosed by transmission electronic microscopy imaging and its hydrodynamic diameter was determined by dynamic light scattering measurement, showing a monodispersed peak at 124.6 ± 1.3 nm, with a polydispersity index of 0.092 (*SI Appendix*, Fig. S1).

The potential of NewPS-mediated aPDT to inactivate Gram-positive bacteria, such as *S. pneumoniae*, was investigated. The culture of *S. pneumoniae* was prepared based on protocols already established (2). The adjustment of the optical density (OD) in a specific wavelength ($\lambda = 600$ nm) was done to guarantee the initial bacteria amount of 10^6 cells/mL. Various concentrations of NewPS (0.5 nM to 100 μM) were added to the bacteria with different incubation times with drug–light intervals (DLI) of 0 min, 20 min, and 1 h for light treatment. Additional samples were incubated with all experimental NewPS concentrations and not exposed to the light ("Only NewPS" Group), to determine the NewPS dark toxicity in comparison with the control group ("Control-Only PBS"). The results demonstrated minimal dark toxicity of the NewPS at the experimental concentration range ($P > 0.5$), independently of the interaction time between the nanoemulsion and the bacteria (*SI Appendix*, Fig. S2).

Regarding the aPDT results, treatment was performed using a light-emitting diode (LED)-based device with wavelength centered at 660 nm and an irradiance of 50 mW/cm^2 and exposure time of 5 and 10 min to give total light fluence of 15 and 30 J/cm^2, respectively. These parameters were performed to both "Only light" and aPDT groups. Fig. 1*A* presents the colony-forming unit (cfu)/mL reduction of *S. pneumoniae*. The "only light" group showed negligible toxicity ($P > 0.5$) under irradiation parameters while aPDT group showed drug–dose and light–fluence enhanced inactivation response.

It was impressive to find out that NewPS-aPDT was able to kill *S. pneumoniae* at a very low NewPS concentration. As shown in Fig. 1*A*, NewPS at 5 nM led to a complete eradication of the microorganism (reduction of more than 6 logs) under all experimental aPDT conditions. NewPS at 2.5 nM presented almost 7 logs of reduction of *S. pneumoniae* when DLI was over 20 min under light fluence of 30 J/cm^2, while it was obtained a reduction of 5 logs with DLI of 0 h. This DLI-dependent effect was clearly demonstrated at the extremely low NewPS concentration of 0.5 nM under 30 J/cm^2 irradiation, where reductions of 6.2, 4.4, and 3.5 logs with the DLI of 1 h, 20 min, and 0 h, respectively, were achieved.

We then tested NewPS-aPDT for the inactivation of the also Gram-positive *S. aureus*, which is one of the most dangerous strains, especially because of its resistance to conventional treatments. In agreement with the absence dark toxicity to *S. pneumoniae*, NewPS at 500 nM did not present any dark toxicity to *S. aureus*, independently of the interaction time between the nanoemulsion and the bacteria.

Downloaded from https://www.pnas.org by Escola Sup Agricultura - USP on November 16, 2022 from IP address 143.107.180.158.

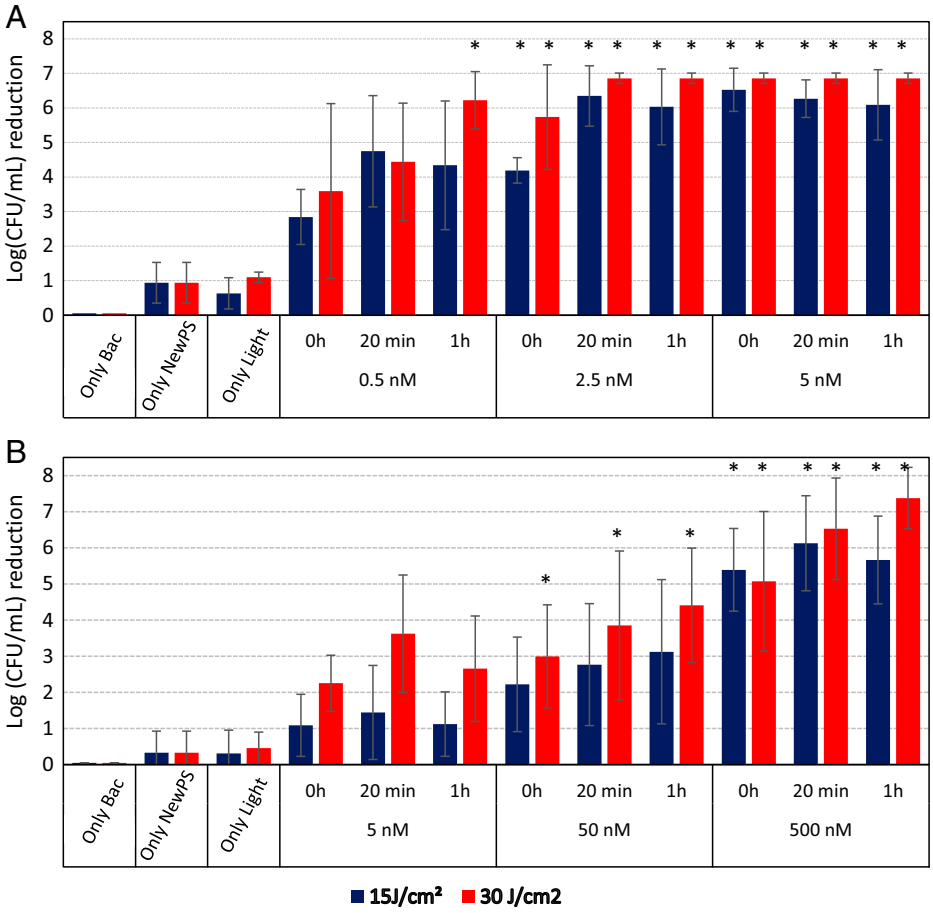

Fig. 1. Reduction in log of cfu/mL using light fluency of 15 and 30 J/cm^2 for planktonic form of (*A*) *S. pneumoniae* and (*B*) *S. aureus*. The DLI was varied in 0, 20 min, and 1 h, and the concentrations showed were 0.5, 2.5, and 5 nM for *S. pneumoniae* and 5, 50, and 500 nM for *S. aureus*. The influence of the DLI for the photodynamic effect is observed, as greater microbial reductions were obtained for longer DLI, comparing the same concentration in both bacterial strains. For *S. pneumoniae*, the potency of NewPS as a photosensitizer for photodynamic inactivation is clear, since with 0.5 nM and 1 h of DLI it is already possible to see a reduction of more than 6 logs. The Control groups (Only PBS, Only NewPS, and Only light) showed almost no effect of reduction (less than 1 log). *Significant differences in comparison to the control group ($P < 0.05$).

Fig. 1*B* shows the cfu/mL reduction of *S. aureus* under NewPS-aPDT, using NewPS at the concentration of 5, 50, and 500 nM, DLI of 0, 20 min, and 1 h, and light fluence of 15 and 30 J/cm^2. Only the light irradiation (in the absence of the PS "only light" group) showed minimal effect against the bacteria ($P > 0.5$). The incubation time of the drug was also found as a main parameter for the effectiveness of aPDT, as the DLI of 0 h presented the lowest reduction compared to DLI of 20 min and 1 h in all conditions evaluated.

In comparison with the reduction obtained in *S. pneumoniae* (6 logs), the 5 nM NewPS achieved a reduction of 3 log in *S. aureus*, which might suggest a higher difficulty to treat *S. aureus* infectious. Nevertheless, increasing the NewPS concentration to 500 nM enabled a reduction of more than 6 logs under 30 J/cm^2 ($P < 0.05$). These data together suggested that NewPS can be a very effective photosensitizer against both type of microorganisms.

aPDT in *S. aureus* biofilm. To further investigate the effectiveness of NewPS-aPDT against biofilm, the *S. aureus* bacteria that showed lower tolerance in the planktonic study was selected to perform this evaluation. First, the distribution of the NewPS within the biofilm was assessed to check its efficacy as a photosensitizer delivery formulation. For this, the porphyrin fluorescence distribution under 10 μM NewPS incubation was monitored at confocal microscopy, collecting z-stack images at the time intervals of 0, 20, 40, and 60 min (Fig. 2*A*). According to the images obtained, it was observed that NewPS was present even at the deeper layers of the biofilm, and the incubation time (DLI) was a fundamental factor for higher and more homogenous distribution of the photosensitizer. The longer the DLI, the greater the penetration of the photosensitizer into the biofilm (Fig. 2*A*). Because the effectiveness of the treatment against biofilm depends on the drug distribution and cell uptake, the confocal images demonstrated that NewPS has the potential for the inactivation of the biofilm cells.

The approach optimization for the biofilm study was proceeded by adjusting the NewPS concentration, incubation time (DLI), single/multi aPDT sessions, and light fluence.

The first trial of NewPS-aPDT in biofilm was conducted by varying NewPS concentrations of 100 nM, 1 μM, and 10 μM and the incubation period (20 min or 1 h of DLI), followed by single aPDT treatment under 30 J/cm^2. However, these aPDT conditions did not present direct significant inactivation response. When 10 μM of NewPS was applied with longer DLI, biofilm viability reduction was observed gradually, and 4 h of DLI resulted in 3.09 and 3.11 log reduction for 30 and 60 J/cm^2, respectively, in comparison with the control group (Fig. 2*B*). Following with the 10 μM of NewPS treatment, when two aPDT sessions with shorter periods of DLI and low light dose was tested, it was consistently observed that longer periods of DLI achieved higher log reductions. The double aPDT sessions with

Downloaded from https://www.pnas.org by Escola Sup Agricultura - USP on November 16, 2022 from IP address 143.107.180.158.

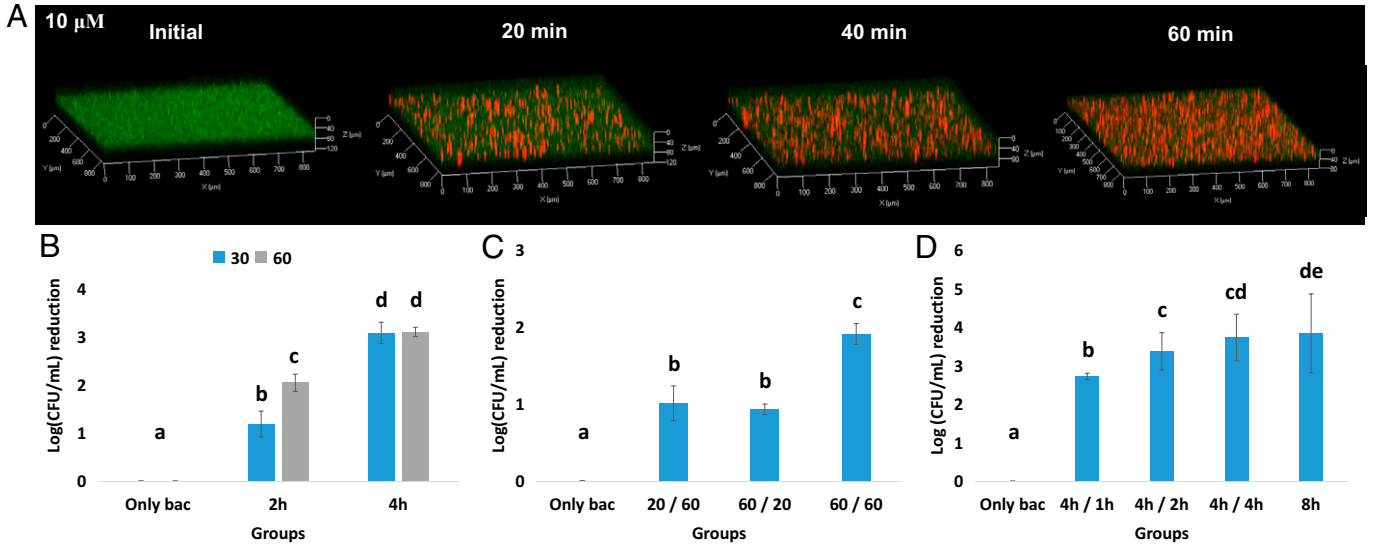

Fig. 2. Fluorescence confocal microscopy images (*A*) and mean values of the biofilm reduction obtained when the NewPS was applied at the concentration of 10 μM (*B*–*D*). (*A*) NewPS penetration at the concentration of 10 μM monitored under confocal microscopy, collecting images at the time intervals of 0, 20, 40, and 60 min. It was observed that NewPS had the ability to achieve deeper layers of the biofilm and the longer the DLI, the greater the penetration of the photosensitizer into the biofilm. (*B*) One aPDT session with DLI of 2 h and 4 h and light doses of 30 and 60 J/cm^2. Biofilm viability reductions were observed gradually, the longer period of incubation resulted in higher viability reductions. The 4 h DLI resulted in 3.09 and 3.11 log reduction for 30 and 60 J/cm^2, respectively, in comparison with the control group. (*C*) Two aPDT sessions with shorter periods of DLI (20 or 60 min) and low light dose (30 J/cm^2). It was observed that longer periods of DLI (60 min) achieved higher log reductions in comparison with the shorter periods of DLI (20 min). The double aPDT sessions with 60 min of DLI used in both sessions were able to reduce 1.91 log of the bacteria. (*D*) A set of two aPDT sessions, with the first session always with the same parameter (4 h of DLI, 30 J/cm^2) and the second session varying the DLI (1, 2, or 4 h of DLI, 30 J/cm^2). The group that combined 4 h of DLI in the first aPDT session followed by 1 h of DLI in the second session resulted in 2.72 of log reduction while that with 2 h of DLI in the second session was able to reduce 3.37 log of the biofilm. The combination of both 4 h of DLI in the first and second aPDT sessions achieved the highest reduction, being equivalent to 3.73 log. Another group of biofilm received a single aPDT session, 8 h of DLI, and 30 J/cm^2 of light, resulting in a reduction of 3.84 log. Lowercase letters indicate significant differences between treatments ($P < 0.05$).

60 min of DLI used in both sessions were able to reduce 1.91 log of the bacteria (Fig. 2*C*). Additionally, another condition of two doses of aPDT was also evaluated, keeping the same parameter for the first session and varying the DLI of the second one. The treatment that combined 4 h of DLI in the first session followed by 1 h of DLI in the second one resulted in 2.72 log reduction while that with 2 h of DLI in the second session was able to reduce 3.37 log of the biofilm. Finally, the combination of both 4 h of DLI in the first and second aPDT sessions achieved the highest reduction, being equivalent to 3.73 log (Fig. 2*D*). In addition, another group of biofilm received a single aPDT session with 8 h of DLI, resulting in a reduction of 3.84 log, as shown in Fig. 2*D*, with significant differences between treatments ($P < 0.05$). These results indicated that, at effective NewPS concentrations, the longer periods of DLI advance the potency of NewPS-aPDT.

Significantly enhanced efficacy of NewPS-aPDT was achieved in biofilm when higher NewPS concentration (100 μM) was applied with longer periods of DLI, in either single or two PDT sessions under higher light doses of 60J/cm^2. The single session protocol evaluated at 2, 4, and 6 h of DLI followed by 60 J/cm^2 of light, and the reductions were equivalent to 3.10, 3.93, and 5.56 logs of the biofilm viability, respectively (Fig. 3*A*). The two aPDT treatment was conducted in biofilm with the first aPDT session varying the DLI (100 μM of NewPS, 1, 2, or 4 h of DLI, and 60 J/cm^2), followed by the second session (100 μM of NewPS, 2 h of DLI, and 60J/cm^2), resulting in the reductions of the biofilm viability by 3.67, 4.52, and 6.03 logs ($P < 0.05$), respectively (Fig. 3*B*). It is important to emphasize that the control biofilms (the only NewPS at 100 μM and the only light at the fluence of 60 J/cm^2) showed viability similar to the untreated biofilms ($P > 0.5$).

In addition to the significant reduction of colony counts demonstrated for NewPS-aPDT, the fluorescence confocal microscopy images also revealed the greatest inactivation achieved with the DLI of 6 h, biofilm received high dose (100 μM of NewPS, 6 h of DLI, and 60 J/cm^2) was subjected to aPDT response analysis by LIVE/DEAD staining under confocal microscopy. The SYTO 9 showed viable bacterial cells signal (excitation/emission, ~495 nm/~515 nm), while propidium iodide (PI) marked dead bacterial cells (excitation/emission, ~490 nm/~635 nm). As shown in Fig. 3*C*, the biofilm initially presented a strong signal of live cells. After 6 h of incubation (before aPDT), NewPS was observed to be well-distributed in biofilm and remained stable after aPDT. Importantly, the biofilm after illumination showed high number of dead cells stained by the PI, (Fig. 3*B*), which strongly support the effectiveness of NewPS-aPDT in biofilm treatment.

Taking all these results into account, it is possible to conclude that longer periods of incubation are crucial for aPDT effectiveness against *S. aureus* biofilm. Furthermore, the best combination was 100 μM with 60 J/cm^2 of light dose achieving a reduction of more than 6 logs, indicating one of the best results in biofilm inactivation found in the literature.

aPDT for In Vivo Model: Infected Ulcers. With the great reduction obtained in the in vitro biofilm, the antimicrobial photodynamic therapy effectiveness was studied in an in vivo infected skin lesion in murine model.

Considering the highest NewPS concentration (100 μM) and the highest light fluence (60 J/cm^2) against biofilm , these parameters were used for the in vivo antimicrobial study against *S. aureus* biofilm present on infected wound of mice. Being the DLI an important parameter for the effectiveness of the treatment, the DLI was varied by 1, 2, and 4 h in asingle aPDT session. Two aPDT sessions were also applied similarly, with 1 h-DLI for each aPDT session. Samples were collected from the infected lesion immediately after and 7 d after aPDT to

Downloaded from https://www.pnas.org by Escola Sup Agricultura - USP on November 16, 2022 from IP address 143.107.180.158.

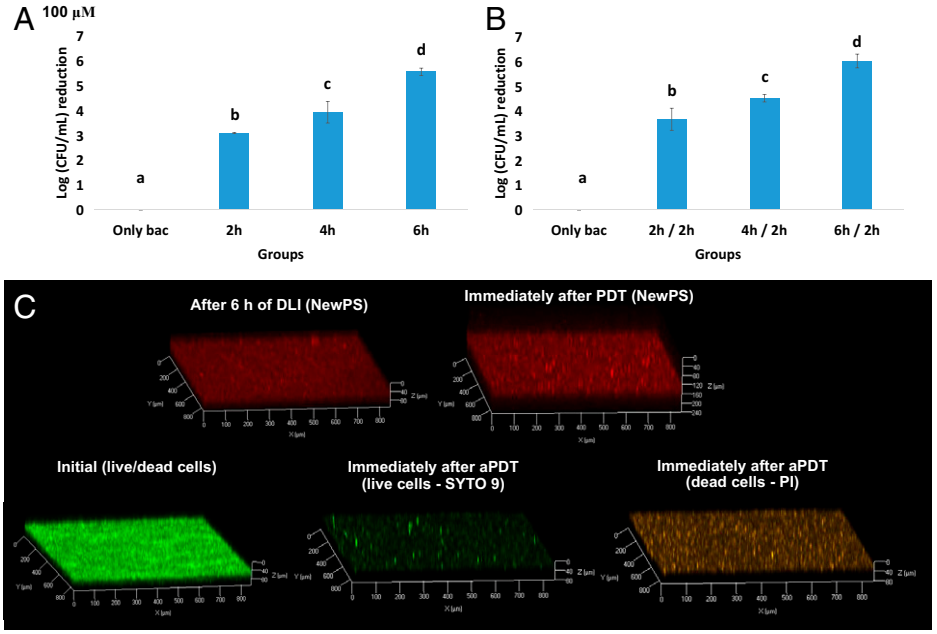

Fig. 3. Mean values of the biofilm reduction (*A* and *B*) and fluorescence confocal microscopy images obtained when the NewPS was applied at the concentration of 100 µM (*C*). (*A*) Single aPDT session mediated by NewPS at the concentration of 100 µM with 2, 4, and 6 h of DLI followed by 60 J/cm^2 of light, which resulted in reductions equivalents to 3.10, 3.93, and 5.56 logs of the biofilm viability, respectively. (*B*) Two aPDT treatments were conducted in biofilm with the first aPDT session varying the DLI (2, 4, or 6 h of DLI and 60 J/cm^2), followed by the second session always with the same parameter (2 h of DLI, 60 J/cm^2). This combination resulted in reductions of 3.67, 4.52, and 6.03 logs, respectively. (*C*) Confocal images obtained with the NewPS at the concentration of 100 µM. On the *Top*, it is possible to observe the NewPS fluorescence and distribution before and after aPDT. On the *Bottom*, the biofilm was stained with SYTO 9 and PI, which show the live and dead cells, respectively. It was possible to verify that initially, the biofilm was composed mainly by live cells. After aPDT, using 100 µM of NewPS, 6 h of DLI, and 60J/cm^2, the biofilm showed high number of dead cells stained by the PI and few live cells. Lowercase letters indicate significant differences between treatments ($P < 0.05$).

determine the bacteria reduction in CFU/mL for different groups and compared with control group (no treatment), Photographs of the lesions were taken before, 3, and 7 d after the aPDT for wound healing evaluation. All results are shown in Fig. 4.

The groups "only light" and "only NewPS" with an incubation time of 2 h were also performed and showed no effect, being similar to the untreated control ($P > 0.5$). For single NewPS-aPDT session, the DLI played essential role for immediately acute response, and the bacteria reduction increased when longer incubation time was used. As shown in Fig. 4, comparing with the control groups, reductions equivalents to <1 logs, 1 and 2 logs were achieved using 1, 2, and 4 h of DLI, respectively ($P < 0.5$). The two aPDT sessions with 1 h of DLI in each session resulted in ∼1 log of reduction immediately after aPDT, being similar to that caused by single aPDT session with 2 h of DLI ($P < 0.5$). These data, together with the planktonic and biofilm results presented previously, suggest that the NewPS incubation time is essential for aPDT effectiveness.

Seven days after treatment, the control group showed a reduction of 2 logs compared to the initial value (baseline) collected ($P < 0.5$), which means that a bacterial reduction is expected due to the host immune response of the mice organism. The "only light" group presented a reduction equivalent to 3 logs (1 log higher than the control) and the "only NewPS" showed a reduction of 2 logs, as the nontreated control group (*SI Appendix*, Fig. S3). The single aPDT with 1 h of DLI resulted in 4 log of reduction, while DLI of 2 h and 4 h and two aPDT sessions enabled a significant reduction of 5–6 logs, with statistical difference ($P < 0.05$), indicating great effectiveness of the NewPS-aPDT for microbial reduction in vivo. Moreover, the single aPDT groups with DLI of 2 and 4 h showed greater tissue recovery than the other groups, especially the nontreated control, indicating that NewPS-aPDT may be considered a simple and safe approach for clinical antimicrobial application. The NewPS properties and the main in vitro (planktonic and biofilm) and in vivo results are summarized in Fig. 5.

Discussion

Drug delivery and antimicrobial response are great challenges in health sciences, due to the high diversity of the microorganism cells and infective forms. An efficient antimicrobial treatment must overcome the resistance provided by the protective biofilm and also the influences by any biological fluid that may be present at the infected lesion. A platform that can efficiently work in such diverse biological conditions is ideal for antibiotics or photosensitizer delivery. In this study, we present NewPS as an efficient nanoemulsion platform for antimicrobial photodynamic therapy.

In the literature, the photodynamic activity of porphyrins against planktonic bacteria is well demonstrated (20). However, high concentrations and fluence levels are often necessary to reduce 6–8 logs of microorganisms, even in planktonic form, which hamper their use in several applications in the clinical routine. Concentrations of 200 µg/mL and a light fluence of 180 J/cm^2 resulted in only 1 log of *S. aureus* reduction (21), while 50 µg/mL and 60 J/cm^2 achieved complete reduction using Photogem in planktonic form (22).

The free photosensitizer molecules are often used in the micromolar order for aPDT against *S. aureus* (23) or *S. pneumoniae* in planktonic form (24). The search for photosensitizers at concentrations in the nanomolar range with high effectiveness has been investigated (25–27). Anionic porphyrins have also been tested and have already shown complete inactivation of planktonic form

Downloaded from https://www.pnas.org by Escola Sup Agricultura - USP on November 16, 2022 from IP address 143.107.180.158.

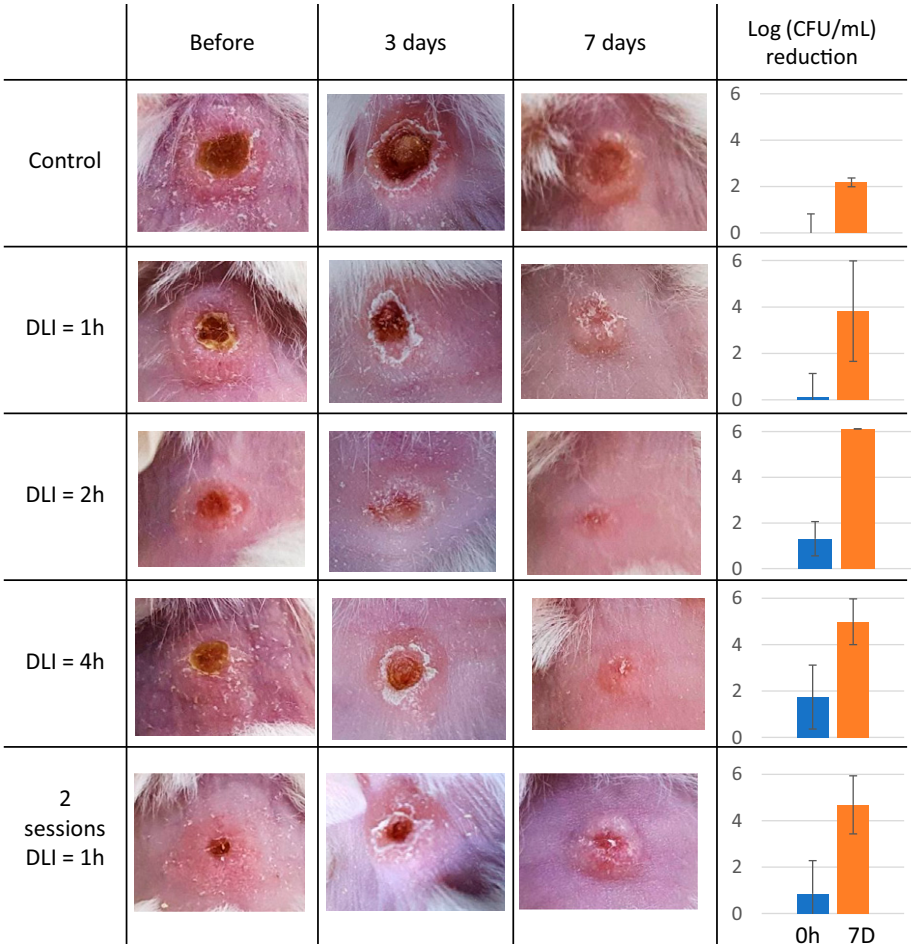

Fig. 4. Infected wounds in mice immediately before, 3 d after, and 7 d after the treatment for different DLI protocols, with 100 μM of NewPS and 60 J/cm^2 and their respective mean reduction in cfu/mL immediately and 7 d after the treatment is shown for each protocol. Immediately after the illumination, it is possible to see a reduction of almost 2 logs in CFU/mL for DLI = 4 h and a reduction of 6 logs after 7 d for DLI = 2 h. For the wound healing process, the DLI of 2 and 4 h showed the best results. It is possible to see a rapid healing process within the first 3 d for these groups, with good healthy tissue after 7 d.

of *S. aureus* with 10 nM (28), while bacteriochlorin and boron dipyrromethene compounds had effect with 100 nM (29, 30). In fact, according to the results obtained, we demonstrated that aPDT using NewPS is highly effective, achieving a reduction of up to 6 log in *S. pneumoniae* and *S. aureus* with the porphyrin nanoemulsion using nanomolar conditions, which indicates a great cell interaction with both Gram-positive and negative bacteria.

Often in vitro studies are performed with pathogen in the planktonic form and can lead to ineffective treatment when transferred to the clinic (1). It is well known that biofilms are less susceptible to PDT when compared to the same pathogen in suspension (11, 31–34). Taking these features into account, biofilms are a challenge for any type of treatment, since they are more virulent and, mainly, because of the presence of the extracellular matrix that difficult the drug penetration, including the photosensitizer uptake by the microorganism cells (35). Another concern for the often incomplete inactivation of biofilm may be related to the heterogeneous photosensitizer distribution, where the photosensitizer does not homogenously distributed within all biofilm layers. A partial inactivation treatment may result in the release of viable cells and further adherence and infection of other surface regions. Thus, improving the photosensitizer delivery and homogeneous distribution, as well as understanding how this happens in a complex structure like the biofilm could be the key for the treatment success. To overcome these photosensitizer challenges and, therefore, the efficiency of aPDT, different strategies of nanoparticle-based photosensitizer delivery have been explored.

Nanoemulsions, a mixture of water, oil, and surfactant, have been applied as nanocarriers of photosensitizer and present several advantages compared to other formulations, such as better solubility, lower toxicity, lower degradation, and also improving their activity. Mainly for drug delivery, nanoemulsions have been used topically to treat local infections (36). NewPS is a simple, versatile, and safe nanoemulsion based on a surfactant-free oil-in-water nanoplatform with a super high capacity of photosensitizer packing (>10 wt%) (19). It has excellent colloidal stability against long term storage (>2 mo), mechanical agitation (80,000 g, 30 min), pH changes (pH2–12, 24 h) and temperature (100 °C, 30 min). Together with its good serum stability and adequate circulation half-life time (slow half-life of 3 h) (19), we believe that NewPS is stable under biofilm administration and topical application on the wound of mouse model. This great stability allows NewPS to permeate through the extracellular matrix until reaching microbial cells even at depth and also in biological fluids that may be present in the infection without losing its properties after hours of incubation. Moreover, its oil matrix is capable of coloading of drugs (e.g., PTX) or antibiotics (e.g., oxacillin, the results will be published separately) enabling further combination or synergistic treatment.

These great characteristics allowed expanding the applications of NewPS for antimicrobial PDT, which was confirmed with the concentration of 0.5 nM resulting in a complete bacteria inactivation against *S. pneumoniae*. Considering the NewPS penetration and, therefore, the aPDT efficacy, an important parameter was the

Downloaded from https://www.pnas.org by Escola Sup Agricultura - USP on November 16, 2022 from IP address 143.107.180.158.

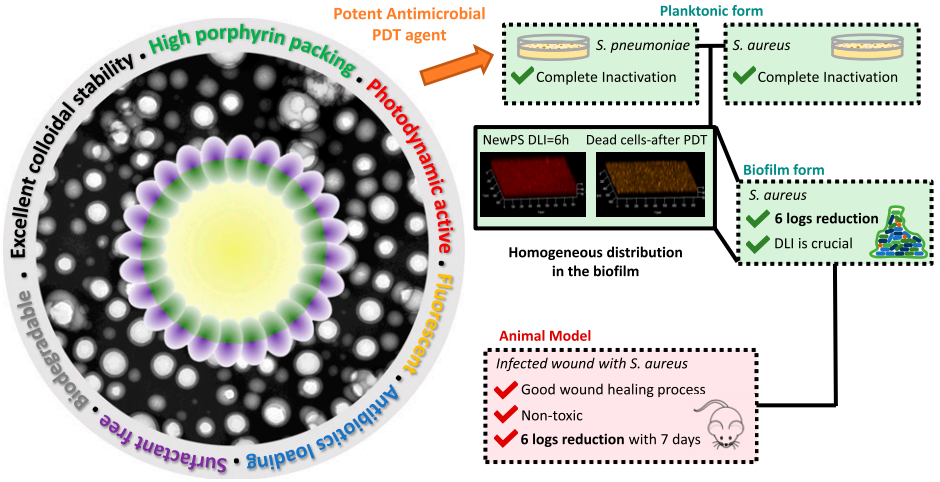

Fig. 5. Summary of NewPS results and its main characteristics, making it a potent PS for antimicrobial application. Highlight for its efficiency in the planktonic, biofilm, and animal model forms, always reaching the same efficiency in log reduction.

time interaction between the photosensitizer and the microorganism cell or the drug-light interval (DLI), as observed in the biofilm and infected wound studies, in agreement with other studies (25). The homogeneous distribution of the photosensitizer, as shown in the confocal microscopy results, may be related to the inactivation of the microorganisms in all layers of the biofilm. It is important to highlight that NewPS showed high interaction the cells in the planktonic form and also a good penetration into all layers of the biofilm, even though it is a system without charges, in contrast with other studies where cationic molecules have shown better antimicrobial activity due to the positive charge (37).

The NewPS property allowed the reduction equivalent to 6.03 log for biofilm, which represents the same reduction of planktonic form. This is a great result in in vitro biofilm models studies, especially comparing this result with studies evaluating aPDT against *S. aureus* biofilm, where reductions between 1 and 4 logs are commonly reported (35, 38).

Another important point is the in vitro biofilm model used in the present study. For biofilm formation, the bacteria were cultured under agitation, which allows a better distribution of the nutrients, facilitates the gas exchanges, and increases the cell circulation, unlike static biofilm formation models. For this reason, the biofilm formed under agitation represents an improved model of a mature biofilm, less tolerant to antimicrobial treatments, to evaluate the translation to in vivo and clinical situation (39, 40).

Furthermore, in a complex organism with its immune system and physical barriers that the tissue itself imposes, the behavior and effectiveness of the treatment can change. Thus, it is of great importance, when proposing a new therapeutic strategy, to test from the planktonic application, through biofilm, and end up in an in vivo study. Taking this into account and considering that the *S. aureus* is the most prevalent strain in infected wounds in the clinic (41), the murine wound model was performed in the present study to analyze the antimicrobial photodynamic action of the NewPS in a complex system. In this case, besides the biofilm condition, there is also present a biological fluid resulting from inflammatory and immune host response, adding another limitation level for the photosensitizer delivery and action.

Several studies with a murine model of infected wounds evaluate different characteristics to study whether a treatment is effective or not, such as the healing process, the reduction of contamination, and the absence of toxicity, with the survival of all treated animals without local edema. Even with the use of other techniques, a reduction of 3 or 4 logs of the microorganism, at the end of the analysis, is already considered an effective antimicrobial treatment (42).

In the present study, reductions of 2 and ~5 logs immediately and 7 d after the treatment, respectively, were observed. In the literature, a study evaluating aPDT in murine model, using light doses of 60 J/cm^2, showed only 3 logs of reductions, 7 d after the treatment (43). In another study, enzyme-activated photodynamic therapy, with 200 μM and 90 J/cm^2, required up to 21 d for complete wound healing infected with *S. aureus* (44). Although some studies show excellent in vitro results, it is not always possible to achieve reductions of up to 6 logs in in vivo studies, even with light doses of 100 J/cm^2 and up to 500 μM of different photosensitizers (45).

Thus, the impressive results obtained in this study, with effectiveness in the nanomolar range for the planktonic form and a reduction of more than 6 logs for the biofilm, turns the NewPS into one of the most promising agents for aPDT studies. Additionally, when tested in an infected tissue model, it proved to be nontoxic to the host tissues. The wound healing process occurred after 7 d with microbial reductions of 2 and 6 logs immediately and 7 d after the treatment, respectively. Therefore, the NewPS formulation showed effective response in the investigated biological environments, including the more complex and challenge ones of biofilm and animal model. For this reason, the NewPS-mediated antimicrobial photodynamic therapy should be considered a highly effective treatment for biofilm-related infections.

Materials and Methods

The design with all parameters tested in this study is summarized in *SI Appendix*, Fig. S4.

Culture Conditions.

***S. pneumoniae*—planktonic form.** A Gram-positive and alpha-hemolytic bacterium (ATC 49619) strain was maintained in brain-heart infusion (BHI, Kasvi) with 15% (vol/vol) glycerol at −80 °C. To perform the assays, samples were grown microaerophillically in BHI at 37 °C until the optical density of the medium, at 600 nm, reached between 0.2 and 0.4, determined in spectrophotometer (Varian Cary 50 UV-Vis Spectrophotometer-Agilent), corresponding to 5×10^7 cfu/mL and 10^9 cfu/mL, respectively. The bacterial cells were harvested by centrifugation and resuspended in phosphate buffered saline (PBS) pH 7.4 with 500 μL of bacteria solution totaling 1×10^7 cfu/mL After all procedures, the solution was serially diluted (1:10) and 10 μL was placed in blood agar plates that were then incubated overnight for CFU counting.

Downloaded from https://www.pnas.org by Escola Sup Agricultura - USP on November 16, 2022 from IP address 143.107.180.158.

***S. aureus*—planktonic form.** *S. aureus* (ATCC 25923) was maintained in BHI supplemented with glycerol (40%) at –20 °C and was reactivated in BHI solid media, and 3 cfu was diluted in 10 mL of BHI liquid media and incubated at 37 °C for 3–4 h until the optical density reached 0.2 (equivalent to 10^8 cells/mL). Subsequently, the bacterial suspension was centrifuged (3000 rpm, 15 min) and resuspended in PBS to correspond to 10^7 cfu/mL

***S. aureus*—biofilm form.** To form the biofilm, the bacteria suspension was prepared as the same way as previously described. Then, 1 mL of the suspension was transferred to a 24-well plate and incubated at 37 °C in a shaker incubator (75 rpm) for 90 min (adhesion phase). After 90 min, the 24-well plate was washed twice with PBS to remove nonadhered cells. Then, 1 mL of tryptic soy broth (TSB) was added to each well. After incubation for 48 h in an orbital shaker (75 rpm) for biofilm formation, the suspension was removed, the biofilms were washed twice with PBS, and the treatments were applied.

Nanoemulsion with a Porphyrin Shell (NewPS). The nanoemulsion was produced as previously described (11). The stock solution at a concentration about 2 mM was kept at 4 °C. For the tests, this stock solution was diluted in PBS and pH 7.4 until the desired concentration, varying from 5 nM to 100 μM.

Light Source. For in vitro tests, a prototype of uniform irradiation for multiwell plates was developed. The device consists of 24 LEDs with emission centered at 660 nm, current controllers and heat dissipation module, emitting light homogeneously where each well receives the equivalent of 50 mW/cm^2. For in vivo tests, a panel of 200 diode lasers centered at 660 nm with a control unit and heat dissipation was also developed. The panel was placed 3 cm above the animal, delivering around 36 mW/cm^2 to the animal's skin. Both light sources were developed by the Technological Support Laboratory (LAT) of São Carlos Institute of Physics, University of Sao Paulo, Brazil.

aPDT and Experimental Groups. To verify the efficacy of NewPS as a photosensitizer against microorganisms, aPDT experiments were conducted in 24-well culture plates containing 500 μL of bacterial suspension with 10^7 cfu/mL and 500 μL of solution with NewPS or PBS, depending of the groups. The control groups were: "Control–only PBS" to compare the normal behavior of each bacterium, "Only light"–with an irradiance of 50 mW/cm^2 and total doses of 15 and 30 J/cm^2, and "Only NewPS"–to analyze the dark toxicity of NewPS, with concentrations varying from 0.5 nM to 100 μM. The incubation time to determine the DLI was investigated for 0 h, 20 min, and 1 h, including for the "Only NewPS" group. For aPDT groups, all concentrations of NewPS were tested with both light doses with all three DLI to find the best protocol for inactivation of *S. pneumoniae*. From the best results for this first microorganism, the parameters were repeated for *S. aureus* with 5, 50, and 500 nM. All groups were made in triplicate on three separate occasions ($n = 9$).

From this, a series of aPDT protocols were evaluated for the biofilms. First, they were incubated for 20 min or 1 h (DLI) with NewPS at the concentrations of 100 nM, 1 μM, and 10 μM of one session of 30 J/cm^2. After this, the 10 μM NewPS was tested at different conditions: one aPDT session with longer periods of DLI (2 or 4 h) and higher light doses (60 J/cm^2), two aPDT sessions with shorter periods of DLI (20 or 60 min) and low light dose (30 J/cm^2), and two aPDT sessions with longer periods (4 h first, followed by 1, 2, or 4 h) of DLI and low light dose (30 J/cm^2). Then, 100 μM of NewPS was tested using higher light doses with longer periods of DLI, in one or two aPDT sessions. All these biofilms' protocols are summarized in the *SI Appendix*, Table S1. Control biofilms corresponded to those that received only NewPS at 100 μM, only light at the dose of 60 J/cm^2, and untreated biofilms.

To calculate the reductions of the groups, the colony count of the experimental group was compared with the count of the control group (microorganism only), considering the difference between the values in log.

Confocal Analysis. The NewPS penetration through the biofilm during the incubation time was monitored under confocal laser scanning microscopy (LSM780, Carl Zeiss). For this, the biofilm was incubated with 10 μM of NewPS and z-stacks images were obtained after 20, 40, and 60 min of incubation. For PS detection, we used 405 and 650 nm of wavelengths for excitation and emission , respectively. Additionally, the bacterial cell viability and the architecture of the biofilm before and after the aPDT treatment were also examined under confocal microscopy, using the best parameters for bacterial inactivation. For this, the biofilm was incubated with 100 μM of NewPS for 6 h, then irradiated with 60 J/cm^2 of red LED light (660 nm). After the treatment, NewPS solution was removed and the biofilm was washed twice with saline. Then, the biofilm was stained using the LIVE/DEAD Baclight Bacterial Viability Kit (Life Technologies GmbH) according to the manufacturer's protocol. This kit is a fluorescence assay based on a mixture of SYTO 9 and PI. The first fluorochrome is a green fluorescent nucleic acid, staining viable bacterial cells, while PI is a fluorescent red nucleic acid that marks nonviable bacterial cells. The mixture of both dyes was added to the biofilm and incubated for 15 min. After this, the dyes were removed, washed with saline and the stained biofilm was imaged, using as excitation/emission wavelengths at 480/500 nm for SYTO-9 stain and 490/635 nm for PI, as recommended by the manufacturers.

Infected Wound in Animal Model. All in vivo studies were approved by Ethics Committee on Animal Use (CEUA) of the Institute of Physics of São Carlos, USP, Brazil (protocol number 9961180121 with an amendment version of July 25, 2021 approved on August 5, 2021).

For the induction of contaminated wounds on the skin of animals, the methodology of Takakura et al. (46) was adapted for 6-wk-old female mice of the Balb-c strain. For immunosuppression, animals received intraperitoneally cyclophosphamide 1 d before and 2 d after wound induction, at a concentration of 150 mg/kg and 100 mg/kg of animal, respectively (47). On the day of the induction, under anesthesia, the wound was produced with the aid of a punch with a diameter of 3 mm. Then, an aliquot of 50 μL of *S. aureus* suspension at 10^7 cfu/mL was inoculated on the region. Treatment procedures were performed 5 d after wound induction, according to each experimental group, with five animals per group.

The microbiological evaluation of the treatment effectiveness was performed immediately after the procedure and 7 d after the end of the treatments through the cell viability test (cfu/mL). For the recovery of microorganisms from the wound of animals, sterile miniswabs, previously soaked in 1 mL of saline solution, were rubbed over the wound of animals for 1 min. Then, the swabs were immersed in Eppendorf microtubes containing 1 mL of saline solution and vigorously shaken to detach the cells from the swab, and serial dilution and plating in BHI Agar was performed. Plates were incubated at 37 °C for 24 h to determine cfu/mL values.

aPDT and In Vivo Experimental Groups. Control groups were made with untreated animals (Control), Only Light, and Only NewPS at 100 μM and aPDT groups using different incubation times. Based on the biofilm parameters, the concentration used was 100 μM with topical application of 50 μL on the lesion, containing the nanoemulsion or saline solution. The wound with the NewPS applied was covered with a sterilized Tegaderm film and a hard aluminum foil prior to light treatment to avoid leakage of the solution from the wound site and light exposure. The DLI was 1, 2, and 4 h, always replacing the NewPS solution every 1 h. The light placement was then controlled precisely only to wound area. One group was performed to analyze the effect of two sessions, with a first DLI of 1 h and the second illumination 1 h after the first one. Illumination was performed immediately before the swab, with a wavelength of 660 nm and a total light dose of 60 J/cm^2. All groups were summarized in *SI Appendix*, Table S2.

Statistical Analysis. The cfu/mL values were transformed into $\log_{10}$. Data were analyzed statistically by one-way analysis of variance and, for multiple comparisons, the post hoc Tukey test was applied ($\alpha = 0.05$). These analyses were performed using the Origin 2018 Academic software.

Data, Materials, and Software Availability. All study data are included in the article and/or *SI Appendix*.

ACKNOWLEDGMENTS. The authors thank Johan Dias, Natalia Inada, and Gabriel Jasinevicius for discussions. Some illustrations were prepared with Biorender.com, and the authors are grateful to the company for this support. The authors acknowledge support from the Fundação de Amparo à Pesquisa do Estado de São Paulo (CEPOF 2013/07276-1, INCT 2014/50857-8, and scholarships FA 2021/01324-0, HHB 2016/14033-6, and GK 2018/18188-0); Conselho Nacional de Desenvolvimento Científico e Tecnológico (INCT 465360/2014-9); CK

Downloaded from https://www.pnas.org by Escola Sup Agricultura - USP on November 16, 2022 from IP address 143.107.180.158.

PQ-CNPq program (305176/2021-8); the University of São Paulo (PUB program grants to A.J.B.T.); the Canadian Institute of Health Research (FDN154326); the Canada Foundation for Innovation (NIF 21765); the Canada Research Chairs Program (950-232468); and the Princess Margaret Cancer Foundation.

Author affiliations: [a]Sao Carlos Institute of Physics, University of Sao Paulo, Sao Carlos, 13566-590, Brazil; [b]Pontificia Universidad Católica de Chile, Institute of Physics, Santiago, 7820436, Chile; [c]Princess Margaret Cancer Centre, University Health Network, Toronto, Ontario, M5G 1L7, Canada; [d]Hagler Fellow, Texas A&M University, College Station, TX, 77843-3126; and [e]Department of Medical Biophysics, University of Toronto, Toronto, Ontario, M5G 1L7, Canada

1. L. Sobotta, P. Skupin-Mrugalska, J. Piskorz, J. Mielcarek, Porphyrinoid photosensitizers mediated photodynamic inactivation against bacteria. *Eur. J. Med. Chem.* **175**, 72–106 (2019).
2. K. Bush *et al.*, Tackling antibiotic resistance. *Nat. Rev. Microbiol.* **9**, 894–896 (2011).
3. M. A. B. Lucien *et al.*, Antibiotics and antimicrobial resistance in the COVID-19 era: Perspective from resource-limited settings. *Int. J. Infect. Dis.* **104**, 250–254 (2021).
4. H. Huang *et al.*, Towards the biofilm characterization and regulation in biological wastewater treatment. *Appl. Microbiol. Biotechnol.* **103**, 1115–1129 (2019).
5. N. Høiby, A personal history of research on microbial biofilms and biofilm infections. *Pathog. Dis.* **70**, 205–211 (2014).
6. P. Gupta, S. Sarkar, B. Das, S. Bhattacharjee, P. Tribedi, Biofilm, pathogenesis and prevention–A journey to break the wall: A review. *Arch. Microbiol.* **198**, 1–15 (2016).
7. R. Wiench, D. Skaba, J. Matys, K. Grzech-Leśniak, Efficacy of toluidine blue–Mediated antimicrobial photodynamic therapy on candida spp. A systematic review. *Antibiotics (Basel)* **10**, 1–17 (2021).
8. B. C. Wilson, M. S. Patterson, The physics, biophysics and technology of photodynamic therapy. *Phys. Med. Biol.* **53**, R61–R109 (2008).
9. R. Ackroyd, C. Kelty, N. Brown, M. Reed, The history of photodetection and photodynamic therapy. *Photochem. Photobiol.* **74**, 656–669 (2001).
10. X. Hu, Y. Y. Huang, Y. Wang, X. Wang, M. R. Hamblin, Antimicrobial photodynamic therapy to control clinically relevant biofilm infections. *Front. Microbiol.* **9**, 1299 (2018).
11. V. Pérez-Laguna *et al.*, Antimicrobial photodynamic activity of Rose Bengal, alone or in combination with Gentamicin, against planktonic and biofilm *Staphylococcus aureus*. *Photodiagn. Photodyn. Ther.* **21**, 211–216 (2018).
12. J. N. Anderl, M. J. Franklin, P. S. Stewart, Role of antibiotic penetration limitation in Klebsiella pneumoniae biofilm resistance to ampicillin and ciprofloxacin. *Antimicrob. Agents Chemother.* **44**, 1818–1824 (2000).
13. W. M. Dunne Jr., E. O. Mason Jr., S. L. Kaplan, Diffusion of rifampin and vancomycin through a *Staphylococcus* epidermidis biofilm. *Antimicrob. Agents Chemother.* **37**, 2522–2526 (1993).
14. C. D. Nadell, K. Drescher, N. S. Wingreen, B. L. Bassler, Extracellular matrix structure governs invasion resistance in bacterial biofilms. *ISME J.* **9**, 1700–1709 (2015).
15. J. Chen *et al.*, Advances in nanomaterials for photodynamic therapy applications: Status and challenges. *Biomaterials* **237**, 119827 (2020).
16. J. M. V. Makabenta *et al.*, Nanomaterial-based therapeutics for antibiotic-resistant bacterial infections. *Nat. Rev. Microbiol.* **19**, 23–36 (2021).
17. S. B. Park *et al.*, Proteomic analysis of antimicrobial effects of pegylated silver coated carbon nanotubes in *Salmonella enterica* serovar Typhimurium. *J. Nanobiotechnology* **16**, 31 (2018).
18. E. Yazar, Y. O. Birdane, K. Yapar, Determination of intracellular (neutrophil and monocyte) concentrations of free and liposome encapsulated ampicillin in sheep. *Vet. Med.* **51**, 51–54 (2006).
19. W. Hou *et al.*, A nanoemulsion with A porphyrin shell for cancer theranostics. *Angew. Chem. Int. Ed. Engl.* **58**, 14974–14978 (2019).
20. I. Stojiljkovic, B. D. Evavold, V. Kumar, Antimicrobial properties of porphyrins. *Expert Opin. Investig. Drugs* **10**, 309–320 (2001).
21. S. Karrer *et al.*, Photodynamic inactivation of staphylococci with 5-aminolaevulinic Acid or photofrin. *Lasers Med. Sci.* **14**, 54–61 (1999).
22. M. M. Gois *et al.*, Susceptibility of *Staphylococcus aureus* to porphyrin-mediated photodynamic antimicrobial chemotherapy: An in vitro study. *Lasers Med. Sci.* **25**, 391–395 (2010).
23. G. Rossi, D. Goi, C. Comuzzi, The photodynamic inactivation of *Staphylococcus aureus* in water using visible light with a new expanded porphyrin. *J. Water Health* **10**, 390–399 (2012).
24. I. S. Leite *et al.*, Near-infrared photodynamic inactivation of S. pneumoniae and its interaction with RAW 264.7 macrophages. *J. Biophotonics* **11**, 1–10 (2018).
25. C. S. Vinagreiro *et al.*, Antibacterial photodynamic inactivation of antibiotic-resistant bacteria and biofilms with nanomolar photosensitizer concentrations. *ACS Infect. Dis.* **6**, 1517–1526 (2020).
26. Y. Arenas *et al.*, Photodynamic inactivation of *Staphylococcus aureus* and methicillin-resistant *Staphylococcus aureus* with Ru(II)-based type I/type II photosensitizers. *Photodiagn. Photodyn. Ther.* **10**, 615–625 (2013).
27. M. Fadel, M. Nasr, R. M. Hassan, S. S. Thabet, Cationic zinc (II) phthalocyanine nanoemulsions for photodynamic inactivation of resistant bacterial strains. *Photodiagn. Photodyn. Ther.* **34**, 102301 (2021).
28. K. O. Wikene, H. V. Rukke, E. Bruzell, H. H. Tønnesen, Physicochemical characterisation and antimicrobial phototoxicity of an anionic porphyrin in natural deep eutectic solvents. *Eur. J. Pharm. Biopharm.* **105**, 75–84 (2016).
29. L. Huang *et al.*, Stable synthetic mono-substituted cationic bacteriochlorins mediate selective broad-spectrum photoinactivation of drug-resistant pathogens at nanomolar concentrations. *J. Photochem. Photobiol. B* **141**, 119–127 (2014).
30. B. L. Carpenter *et al.*, Antiviral, antifungal and antibacterial activities of a BODIPY-based photosensitizer. *Molecules* **20**, 10604–10621 (2015).
31. F. Giuliani *et al.*, In vitro resistance selection studies of RLP068/Cl, a new Zn(II) phthalocyanine suitable for antimicrobial photodynamic therapy. *Antimicrob. Agents Chemother.* **54**, 637–642 (2010).
32. C. Vassena *et al.*, Photodynamic antibacterial and antibiofilm activity of RLP068/Cl against *Staphylococcus aureus* and *Pseudomonas aeruginosa* forming biofilms on prosthetic material. *Int. J. Antimicrob. Agents* **44**, 47–55 (2014).
33. M. Wu *et al.*, Disinfection of cariogenic pathogens in planktonic lifestyle, biofilm and carious dentine with antimicrobial photodynamic therapy. *Photochem. Photobiol.* **96**, 170–177 (2020).
34. A. P. D. Ribeiro *et al.*, Photodynamic inactivation of planktonic cultures and biofilms of *Candida albicans* mediated by aluminum-chloride-phthalocyanine entrapped in nanoemulsions. *Photochem. Photobiol.* **89**, 111–119 (2013).
35. A. C. Zangirolami *et al.*, Avoiding ventilator-associated pneumonia: Curcumin-functionalized endotracheal tube and photodynamic action. *Proc. Natl. Acad. Sci. U.S.A.* **117**, 22967–22973 (2020).
36. A. L. P. Silvestre *et al.*, Current applications of drug delivery nanosystems associated with antimicrobial photodynamic therapy for oral infections. *Int. J. Pharm.* **592**, 120078 (2021).
37. J. Oyim, C. A. Omolo, E. K. Amuhaya, Photodynamic antimicrobial chemotherapy: Advancements in porphyrin-based photosensitize development. *Front Chem.* **9**, 635344 (2021).
38. A. D. Verderosa, M. Totsika, K. E. Fairfull-Smith, Bacterial biofilm eradication agents: A current review. *Front Chem.* **7**, 824 (2019).
39. E. Thiran *et al.*, Biofilm formation of *Staphylococcus aureus* dairy isolates representing different genotypes. *J. Dairy Sci.* **101**, 1000–1012 (2018).
40. S. Stepanović, D. Vuković, P. Jezek, M. Pavlović, M. Svabic-Vlahović, Influence of dynamic conditions on biofilm formation by staphylococci. *Eur. J. Clin. Microbiol. Infect. Dis.* **20**, 502–504 (2001).
41. R. Serra *et al.*, Chronic wound infections: The role of *Pseudomonas aeruginosa* and *Staphylococcus aureus*. *Expert Rev. Anti Infect. Ther.* **13**, 605–613 (2015).
42. M. S. Mulani, E. E. Kamble, S. N. Kumkar, M. S. Tawre, K. R. Pardesi, Emerging strategies to combat ESKAPE pathogens in the era of antimicrobial resistance: A review. *Front. Microbiol.* **10**, 539 (2019).
43. O. Simonetti *et al.*, Effectiveness of antimicrobial photodynamic therapy with a single treatment of RLP068/Cl in an experimental model of *Staphylococcus aureus* wound infection. *Br. J. Dermatol.* **164**, 987–995 (2011).
44. X. J. Fu *et al.*, Enzyme activated photodynamic therapy for methicillin-resistant *Staphylococcus aureus* infection both in vitro and in vivo. *J. Photochem. Photobiol. B* **136**, 72–80 (2014).
45. G. Fila *et al.*, Murine model imitating chronic wound infections for evaluation of antimicrobial photodynamic therapy efficacy. *Front. Microbiol.* **7**, 1258 (2016).
46. N. Takakura *et al.*, A novel murine model of oral candidiasis with local symptoms characteristic of oral thrush. *Microbiol. Immunol.* **47**, 321–326 (2003).
47. W. W. Wicha, D. B. Strickmann, S. Paukner, Pharmacokinetics/pharmacodynamics of lefamulin in a neutropenic murine pneumonia model with *Staphylococcus aureus* and *Streptococcus pneumoniae*. *J. Antimicrob. Chemother.* **74** (suppl. 3), iii11–iii18 (2019).

Downloaded from https://www.pnas.org by Escola Sup Agricultura - USP on November 16, 2022 from IP address 143.107.180.158.